

Blue Organic Light-Emitting Diodes Based on Diarylamino-Substituted Stilbene Derivatives

SUNG MIN KWON,¹ KUM HEE LEE,¹ HYUCK JOO KWON,²
YOUNG KWAN KIM,^{2,*} AND SEUNG SOO YOON^{1,*}

¹Department of Chemistry, Sungkyunkwan University, Suwon 440-746, Korea

²Department of Information Display, Hongik University, Seoul 121-791, Korea

A series of diarylamino-substituted stilbene derivatives with various aromatic system were synthesized. multilayered OLEDs with the configuration of ITO/NPB (700 Å)/ADN: blue dopants 1–5 (300 Å: 2 %)/Alq3 (300 Å)/Liq (10 Å)/Al were fabricated. All devices showed the efficient blue emissions. Among these devices, the devices using 4,4'-bis(9,9-diethylfluoren-2-yl)-3,5-di-tert-butylphenylamino)stilbene 4 as a dopant exhibited blue emission with the luminance of 12590 cd/m², the luminous efficiency of 9.10 cd/A at 20 mA/cm², the power efficiency of 3.73 lm/W at 20 mA/cm², and the CIE coordinates of (0.155, 0.195) at 10.0 V.

Keywords Blue fluorescent dopant; buchwald-hartwig cross-coupling; electroluminescence; OLEDs; stilbene derivatives

Introduction

Organic light-emitting diodes (OLEDs) have received considerable the next generation flat-panel display because OLEDs have the advantages of low-driving-voltage, high efficiency, and possibility for flexible and large-area display applications [1]. Red, green, and blue are needed to obtain a full-color display. While a larger number of exceptional red and green emitters have been developed that satisfy the requirements for OLEDs, efficient and stable organic blue emitters are still rare. During the past decades, great efforts were focused on the development of high-performance blue electroluminescent materials with desirable properties, because the improved efficiency, raised color purity, and extended operation lifetime are difficult due to their wide energy band gap. Thus, several efficient blue emitters have been developed, including metal-complexes [2], distyrylarylenes [3,4], oligofluorenes [5], spirobifluorenes [6,7], carbazoles [8], and others [9–13]. However, the electroluminescent properties of blue emitters are necessary to improve full color display performance.

*Address correspondence to S.S. Yoon, Department of Chemistry, Sungkyunkwan University, Cheoncheon-dong, Jangan-gu, Suwon, 440-746, Korea (ROK). Tel: (+82) 31-290-5971; Fax: (+82) 31-290-7075. E-mail: ssyoon@skku.edu; or Y. K. Kim, Department of Information Display, Hongik University, Mapo-gu, Sangsu-dong, Seoul 121-791, Korea (ROK). Tel: (+82)2-320-1646. Fax: (+82)2-3141-8928. E-mail: kimyk@hongik.ac.kr

Stilbene derivatives have attracted great interests in the area of OLED because these materials are well known to exhibit blue photoluminescence by themselves and have promising photoluminescent and electroluminescent properties [16]. Particularly, diarylamino-substituted stilbene derivatives possess the great promise for the efficient blue OLED, because the diaryamine moieties improve the hole transport properties [17,18] through the effective conjugation with the stilbene core [14] as well as the fluorescent quantum yield through a significant decrease of the quantum yields for cis-trans photoisomerization [15].

In this paper, we have designed and synthesized a new class of blue emitter **1–5** based on bis(diarylamino)stilbene derivatives [19]. In these molecules, various arylamine groups are introduced at the 4- and 4'-positions of the central stilbene core to test substituent effect on the electroluminescent performances. In addition, we expected that the introduction of a sterically bulky tert-butyl unit might reduce degree of intermolecular π - π stacking and concentration quenching, leading to the improved EL performances. Herein, synthesis and electroluminescent properties of these new materials when doped in the suitably matched host in the emitting layer of an OLED are described.

Experimental

Synthesis

4,4'-bis(3,5-di-*tert*-butylphenylamino)stilbene (**6**): 4,4'-Dibromostilbene (2.10 g, 6.21 mmol), 3,5-di-*tert*-butylaniline (2.68 g, 13.0 mmol), Pd₂dba₃ (0.285 g, 0.31 mmol), (2-biphenyl)di-*tert*-butylphosphine (0.185 g, 0.62 mmol), sodium *tert*-butoxide (2.38 g, 24.8 mmol), and toluene (30 mL) were charged in a two-necked flask kept under nitrogen. The mixture was heated at reflux for 18 h. After cooling, the solvent was removed under vacuum and the residue was extracted with dichloromethane/water. The organic layer was dried over MgSO₄ and filtered. The residue obtained after evaporation of the solvent was recrystallized from dichloromethane/hexane. Compound **6** was obtained as a bright green solid in 52.6% yield. ¹H-NMR (300 MHz, CDCl₃) [δ ppm]: 7.39 (d, *J* = 8.5 Hz, 4H), 7.04–6.93 (m, 12H), 5.81 (s, 2H), 1.32 (s, 36H). ¹³C-NMR (75 MHz, CDCl₃) [δ ppm]: 152.2, 143.2, 141.9, 127.5, 117.1, 116.1, 113.5, 35.2, 31.7. FT-IR [ATR]: ν = 3420, 3029, 2965, 1592, 1517, 1449, 1335, 968, 849, 708 cm⁻¹. EI-MS (*m/z*): 587 [M⁺].

General procedure for the Synthesis of Compound (1–5): To a toluene (15 mL) solution of 4, 4'-bis(3,5-di-*tert*-butylphenylamino)stilbene (500 mg, 0.85 mmol) were added corresponding aryl bromide (2.13 mmol), sodium *tert*-butoxide (327 mg, 3.41 mmol), Pd₂dba₃ (39 mg, 0.043 mmol), and (2-biphenyl)di-*tert*-butylphosphine (25 mg, 0.085 mmol) under nitrogen. The resulting solution was heated to reflux for 18 h. The solution mixture was extracted with toluene and washed twice with water. The combined organic layers were dried over MgSO₄ and the solvent removed under reduced pressure to afford a crude product that was purified by column chromatography on silica gel using a mixture dichloromethane/hexane (1:4) as the eluent.

4,4'-bis(4-trimethylsilylphenyl)-3,5-di-*tert*-butylphenylamino)stilbene (**1**): Bright green solid. Yield: 39.9 %. ¹H-NMR (300 MHz, CDCl₃) [δ ppm]: 7.37–7.34 (m, 8H), 7.13 (s, 2H), 7.08–7.03 (m, 8H), 6.97–6.96 (m, 6H), 1.25 (s, 36H), 0.25 (s, 18H). ¹³C-NMR (75 MHz, CDCl₃) [δ ppm]: 152.0, 148.5, 147.2, 146.6, 134.3, 132.9, 131.9, 127.2, 126.8, 124.1, 122.2, 120.3, 117.9, 35.2, 31.7, 0.7. FT-IR [ATR]: ν = 2956, 1511, 1321, 1216, 1109, 829, 751, 713, 683 cm⁻¹. FAB-MS (*m/z*): 882 [M⁺]. HRMS-TOF (M⁺+H) Anal. calcd for C₆₀H₇₉N₂Si₂ 883.5782; found: 883.5767.

4,4'-bis(4-methoxyphenyl-3,5-di-*tert*-butylphenylamino)stilbene (**2**): Bright green solid. Yield: 43.5%. ¹H-NMR (300 MHz, CDCl₃) [δ ppm]: 7.31 (d, J = 8.4 Hz, 4H), 7.11–7.05 (m, 6H), 6.98–6.92 (m, 10H), 6.83 (d, J = 8.8 Hz, 4H), 3.81 (s, 6H), 1.24 (s, 36H). ¹³C-NMR (75 MHz, CDCl₃) [δ ppm]: 156.2, 151.8, 147.9, 147.2, 141.0, 130.7, 127.4, 127.0, 126.2, 121.9, 118.8, 116.8, 114.8, 55.7, 35.1, 31.7. FT-IR [ATR]: ν = 2967, 1589, 1505, 1301, 1239, 1035, 825, 711 cm⁻¹. FAB-MS (m/z): 798 [M⁺]. HRMS-TOF (M⁺+H) Anal. calcd for C₅₆H₆₇N₂O₂ 799.5203; found: 799.5189.

4,4'-bis(2-naphthyl-3,5-di-*tert*-butylphenylamino)stilbene (**3**): Bright green solid. Yield: 42.3 %. ¹H-NMR (500 MHz, CDCl₃) [δ ppm]: 7.75 (d, J = 7.5 Hz, 2H), 7.70 (d, J = 8.5 Hz, 2H), 7.59 (d, J = 8.5 Hz, 2H), 7.46 (s, 2H), 7.40–7.32 (m, 8H), 7.30 (dd, J = 2.0, 9.0 Hz, 2H), 7.14 (s, 2H), 7.09 (s, 4H), 6.99 (s, 2H), 1.25 (s, 18H). ¹³C-NMR (75 MHz, CDCl₃) [δ ppm]: 152.1, 147.5, 146.9, 145.7, 134.7, 131.9, 130.2, 128.9, 127.8, 127.3, 127.2, 126.8, 126.4, 124.7, 124.5, 123.8, 120.1, 119.9, 117.7, 35.2, 31.7. FT-IR [ATR]: ν = 3028, 2965, 1589, 1509, 1306, 961, 839, 750, 714, 659 cm⁻¹. FAB-MS (m/z): 838 [M⁺]. HRMS-TOF (M⁺ + H) Anal. calcd for C₆₂H₆₇N₂ 839.5304; found: 839.5266.

4,4'-bis(9,9-diethylfluoren-2-yl-3,5-di-*tert*-butylphenylamino)stilbene (**4**): Bright green solid. Yield: 46.5 %. ¹H-NMR (500 MHz, CDCl₃) [δ ppm]: 7.62 (d, J = 7.5 Hz, 2H), 7.57 (d, J = 8.0 Hz, 2H), 7.36 (d, J = 9.0 Hz, 4H), 7.32–7.27 (m, 4H), 7.24–7.23 (m, 2H), 7.11–7.06 (m, 10H), 6.98 (s, 6H), 1.99–1.87 (m, 8H), 1.24 (s, 36H), 0.34 (t, J = 7.0 Hz, 12H). ¹³C-NMR (75 MHz, CDCl₃) [δ ppm]: 151.8, 151.3, 149.9, 147.7, 147.4, 147.1, 141.7, 136.8, 131.5, 127.2, 127.1, 126.6, 126.5, 123.9, 123.4, 123.0, 120.4, 119.5, 119.3, 119.0, 117.0, 56.4, 35.1, 33.0 31.6. FT-IR [ATR]: ν = 2970, 1502, 1460, 1366, 1217, 1033, 738, 661 cm⁻¹. FAB-MS (m/z): 1026 [M⁺]. HRMS-TOF (M⁺+H) Anal. calcd for C₇₆H₈₇N₂ 1027.6869; found: 1027.6866.

4,4'-bis[(3,5-di-*tert*-butylphenyl)-4-biphenylamino]stilbene (**5**): Bright green solid. Yield: 34.3 %. ¹H-NMR (300 MHz, CDCl₃) [δ ppm]: 7.60 (d, J = 7.2 Hz, 4H), 7.48 (d, J = 8.7 Hz, 4H), 7.44–7.37 (m, 8H), 7.31 (d, J = 7.3 Hz, 2H), 7.18–7.08 (m, 10H), 7.01–6.98 (m, 6H), 1.26 (s, 36H). ¹³C-NMR (75 MHz, CDCl₃) [δ ppm]: 152.1, 147.3, 146.8, 140.9, 124.9, 131.9, 129.0, 127.8, 127.3, 127.0, 126.9, 126.7, 123.9, 123.8, 120.0, 117.7, 35.2, 31.7. FAB-MS (m/z): FT-IR [ATR]: ν = 3031, 2969, 1598, 1487, 1364, 1321, 966, 827, 758, 693 cm⁻¹. FAB-MS (m/z): 890 [M⁺]. HRMS-TOF (M⁺+H) Anal. calcd for C₆₆H₇₁N₂ 891.5617; found: 891.5583.

Fabrication of OLED

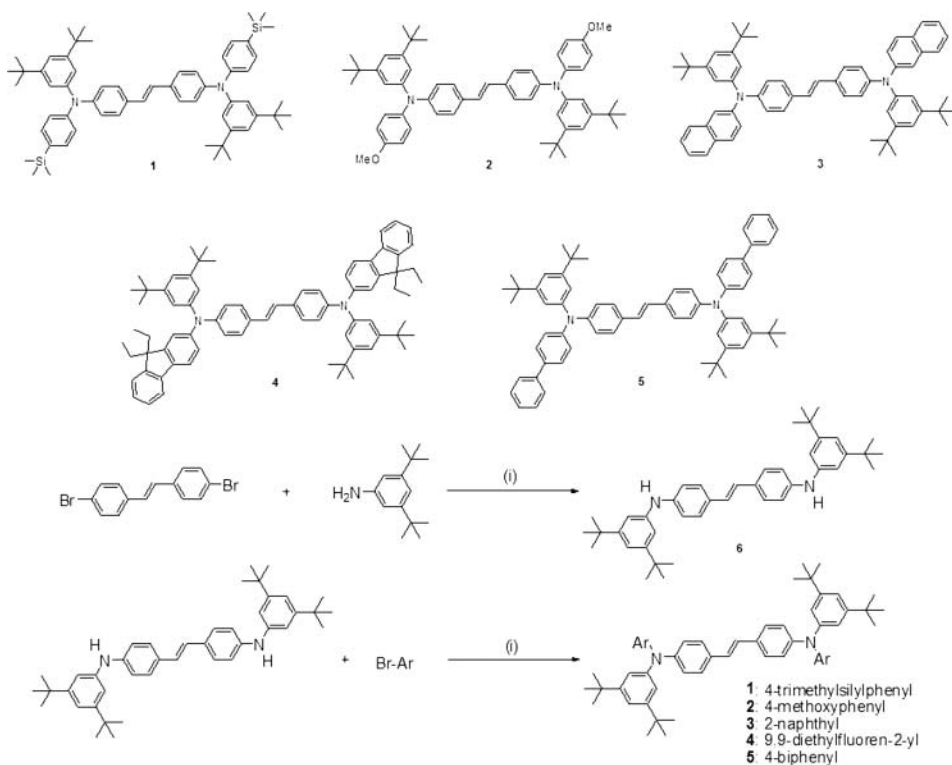
For fabricating OLEDs, indium-tin-oxide (ITO) thin films coated on glass substrates were used, which were 30 Ω /square of the sheet resistivity. The ITO-coated glass was cleaned in an ultrasonic bath by the following sequences: acetone, methyl alcohol, distilled water, storage in isopropyl alcohol for 48 h, drying by an N₂ gas gun. The substrates were treated by O₂ plasma treatment at 2×10^{-2} Torr at 125 W for 2 min. All organic materials and metals were deposited under high vacuum (5×10^{-7} Torr). The OLEDs fabricated in this study had a configuration of indium tin oxide (ITO)/4,4'-bis[N-(1-naphthyl)-N-phenylamino]biphenyl (NPB) (700 Å)/9,10-di(2-naphthyl)anthracene (ADN): blue dopants 1–3 (300 Å: 2%)/tris(8-hydroxyquinolino)aluminum (Alq₃) (300 Å)/lithium quinolate (Liq) (10 Å)/Al. All of the optical and electrical properties of OLEDs such as the current density, luminance, luminous efficiency and CIE coordinate characteristics were measured with Keithly 236, LS-50B, and MINOLTA CS-100A, respectively.

Measurements

All reactions were performed under a nitrogen atmosphere. Commercially available reagents and solvents were used without further purification unless otherwise noted. ^1H - and ^{13}C - NMR spectra were recorded on a Varian (Unity Inova 300Nb or Unity Inova 500Nb) spectrometer. FT-IR spectra were recorded using a Bruker VERTEX70 FT-IR spectrometer. Low- and high- resolution mass spectra were measured using a Jeol JMS-AX505WA spectrometer in FAB mode or Jeol JMS-600 spectrometer in EI mode and a JMS-T100TD (AccuTOF-TLC) in the positive ion mode.

The UV-Vis absorption measurements of these blue compounds in dichloromethane (10^{-5} M) were acquired with a Sinco S-3100 in a quartz cuvette (1.0 cm path). Photoluminescence spectra were measured on an Amincobrowman series 2 luminescence spectrometer. The fluorescence quantum yields of the blue materials were determined in dichloromethane at 293 K against BDAVBi as a reference ($\Phi = 0.86$) [20].

HOMO (highest occupied molecular orbital) energy levels were determined with a low energy photoelectron spectrometer (Riken-Keiki, AC-2). The energy band gaps were determined from the intersection of the absorption and photoluminescence spectra. LUMO (lowest unoccupied molecular orbital) energy levels were calculated by subtracting the corresponding optical band gap energies from the HOMO energy values.



Scheme 1. Molecular structures and synthetic route for bis(diarylamino)stilbene derivatives.

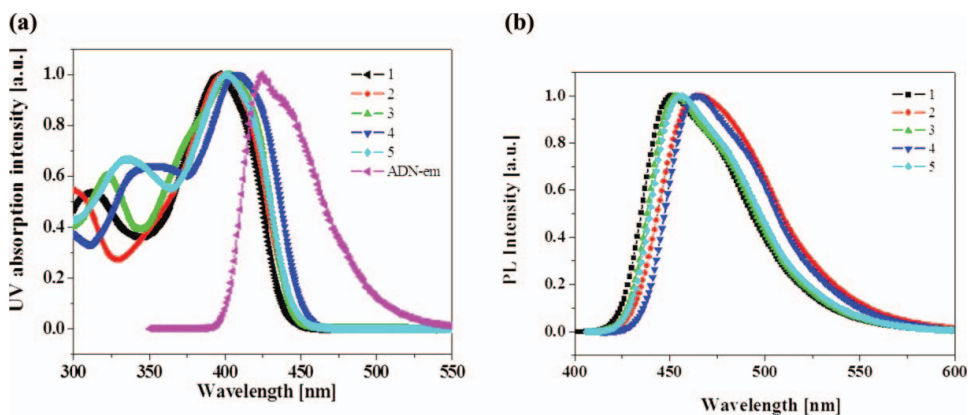


Figure 1. (a) Absorption and (b) emission spectra of blue-light-emitting materials **1–5** in dichloromethane solution.

Results and Discussion

The development of palladium-catalyzed aromatic carbon-nitrogen bond formation provides a feasible method for synthesis of N-diarylamino-substituted stilbenes. As is shown in Scheme 1, the Pd₂dba₃/(2-biphenyl)di-*tert*-butylphosphine/NaO^tBu catalyst system was employed for the coupling of *trans*-4,4'-bis(3,5-di-*tert*-butylphenylamino)stilbene and corresponding aryl bromides to afford compounds **1–5**. To investigate the influence of the aromatic end groups, five designed compounds introduced end groups with various aromatic units. Compounds **1–5** had 4-trimethylsilylphenyl, 4-methoxyphenyl, 2-naphthyl, 9,9-diethylfluoren-2-yl, and 4-biphenyl end group, respectively. The molecular structures of the compounds were characterized by ¹H- and ¹³C-NMR, FR-IR, and low- and high-resolution mass spectroscopy.

The UV-Vis absorption spectra of these blue fluorescent materials in dichloromethane are shown in Fig. 1(a). Also, the photophysical data are summarized in Table 1. Compounds **1–5** show a main absorption peak at 396–408 nm range and good spectral overlap was observed between the emission of the host (ADN) and the absorption of the dopant materials **1–5**. These observations indicate that the blue materials **1–5** can effectively accept energy from the ADN host material by Förster-type energy transfer. A particularly good spectral overlap was observed in the dopant **4**. The energy transfer efficiency is highly dependent on the spectral overlap between the emission of the host and the absorption of the dopant, so this material should be expected to have highly efficient electroluminescent properties in OLED devices.

The normalized PL emission spectra of the compounds **1–5** are shown in Fig. 1(b). All materials showed blue fluorescence with maximum emission wavelengths at 451, 465, 454, 464, and 456 nm, respectively. A comparison of the emission wavelengths of compound **4** and **5** clearly indicates that the planar biphenyl unit of the outer fluorene in the former is easy to the electron delocalization between N-aryl and aminostilbene groups. Compound **5** broke the conjugation system due to the distorted structure at the biphenyl units. Consequently, the energy gaps of compound **4** decreased while the absorption/emission peaks were red-shifted in comparison with compound **5**. The FWHM of the spectra is very narrow at 58–65 nm, and these blue-light-emitting bis(diarylamino)stilbene derivatives have high PL

Table 1. Photophysical data of compounds **1–5**

Compound	Abs λ_{max} [nm] [a]	PL λ_{max} [nm] [b]	FWHM [nm]	HOMO [eV] [c]	LUMO [eV] [c]	Bandgap [eV]	Φ [d]
1	396	451	59	−5.32	−2.44	2.88	0.98
2	399	465	65	−5.25	−2.41	2.84	0.82
3	403	454	58	−5.17	−2.32	2.85	0.85
4	408	464	59	−5.29	−2.49	2.80	0.67
5	401	456	58	−5.38	−2.53	2.85	0.75

[a,b] Maximum absorption and emission wavelength, measured in CH_2Cl_2 solution, [c] Obtained from AC-2 and the intersection of the absorption and photoluminescence spectra, [d] Using BDAVB_i as a standard; $\lambda_{\text{ex}} = 360$ nm ($\Phi = 0.86$ in CH_2Cl_2).

quantum yields of 0.67–0.98, suggesting that these materials are expected to have highly efficient electroluminescent properties in OLED devices.

The highest occupied molecular orbital (HOMO) and lowest unoccupied molecular orbital (LUMO) energy levels of compounds **1–5** are shown in Table 1. The HOMO energy levels were measured with an AC-2 photoelectron spectrometer and the LUMO levels calculated by subtracting the corresponding optical band gap energies from the HOMO values. The HOMO/LUMO energy levels of compounds **1–5** are −5.32/−2.44, −5.25/−2.41, −5.17/−2.32, 5.29/−2.49, and −5.38/−2.53, respectively. Also the optical band gap calculated from the threshold of optical absorption are 2.88 eV, 2.84 eV, 2.85 eV, 2.80 eV and 2.85 eV, respectively. The energy levels are sensitive to aryl substituents at the 4- and 4'-positions of the stilbene core. It is expected that the introduction of the two electron-donor methoxy groups can raise the HOMO energy level of the compound. Compared to compound **1** with same aromatic framework, resonance effects provided directly by lone-pair electrons in compound **2** will have stronger influence than the electronic inductive effect of substituents in increase HOMO level. In fact, compared to the PL spectrum and energy level of **1**, those of **2** indicated red shifts of 14 nm and higher HOMO level due to the introduction of two methoxy groups.

To explore the electroluminescent properties of these molecules, devices were fabricated with a structure of ITO/NPB (700 Å)/ADN: Blue dopants **1–5** (300 Å)/Alq₃ (300 Å)/Li_q (20 Å)/Al and their electroluminescent performance characteristics of devices are summarized in Table 2. The doping concentrations of **1–5** in ADN were optimized to 2%, respectively. As shown in Fig. 2, the energy barrier between the HTL and EML is 0.3 eV, while that between ETL and EML is 0.7 eV. This suggests that the device should allow more efficient hole injection than electron injection into the EML. Also, it is well recognized that the mobility of holes is much higher than that of electrons [21]. Consequently, holes tend to transport easily to the ETL without recombining efficiently with electrons in the emissive layer. To confine and enhance electron-hole recombination in the EML and thus to increase device efficiency, a hole-transport layer thickness (70 nm) fabricated more than two times that of the electron-transport layer (30 nm).

The EL emission spectra of the devices **1–5** with emitting layers consisting of the ADN host doped with dopants **1–5** are seen in Fig. 3. All five stilbene-based devices exhibited blue emissions with maximum emission peaks between 452–482 nm. The corresponding CIE coordinates are $x = 0.158$, $y = 0.177$ for **1**, $x = 0.174$, $y = 0.264$ for **2**, $x = 0.154$, $y = 0.185$ for **3**, $x = 0.155$, $y = 0.195$ for **4**, and $x = 0.170$, $y = 0.224$ for **5**. Figure 4

Table 2. Electroluminescence characteristics of OLEDs based on blue dopant materials **1–5**

Compound	Max. luminance [cd m ⁻²]	Luminance, Efficiency		Max. efficiency [cd A ⁻¹ , lm W ⁻¹]	Lifetime [h] [b]	Emission λ_{max} [nm]	CIE coordinates [x, y]
		Efficiency [cd m ⁻² , cd A ⁻¹ , lm W ⁻¹] [a]	Efficiency [lm W ⁻¹] [a]				
1	7207	1218, 6.10, 2.39		6.65, 3.38	263	452/476	0.158, 0.177
2	8252	1469, 7.35, 2.89		8.37, 4.48	212	486	0.174, 0.264
3	14810	1443, 7.23, 3.21		7.39, 3.98	76	464	0.154, 0.185
4	12590	1814, 9.10, 3.74		9.66, 5.35	162	458/482	0.155, 0.195
5	10540	1529, 7.66, 3.15		7.79, 3.88	124	476	0.170, 0.224

[a] At current density of 20 mA cm⁻², [b] at $L/L_0 = 0.7$ under initial luminance 4000 cd m⁻².

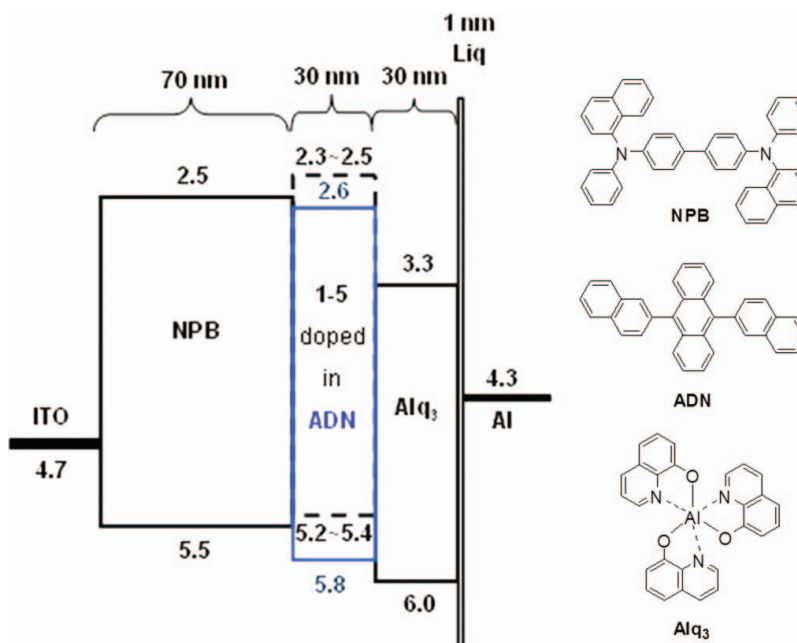


Figure 2. Relative energy-level alignments and layer thickness of OLEDs.

shows the operational lifetime of these blue devices. The measured lifetime of devices 1–5 at $L/L_0 = 0.7$ were 263, 212, 76, 162, and 124 h at an initial luminance of 4000 cd m^{-2} , respectively. Renormalizing to a initial luminance of 100 cd m^{-2} , the lifetimes of devices 1–5 were measured to be 10500, 8480, 3040, 6480, and 4960 h, respectively. Interestingly, device 3 employing 3 as a dopant with the higher LUMO and HOMO level than the others showed the worst device operational lifetime.

Figure 5(a) and (b) shows the luminance-voltage and current density-voltage characteristics of the devices containing ADN doped with various dopant materials. The maximum

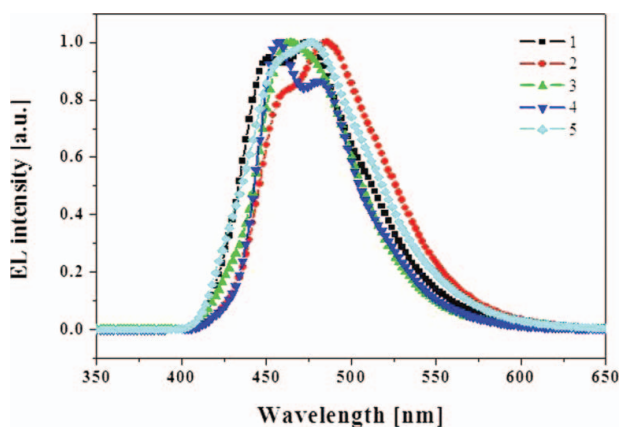


Figure 3. EL spectra of devices using the five stilbene derivatives as dopant emitters.

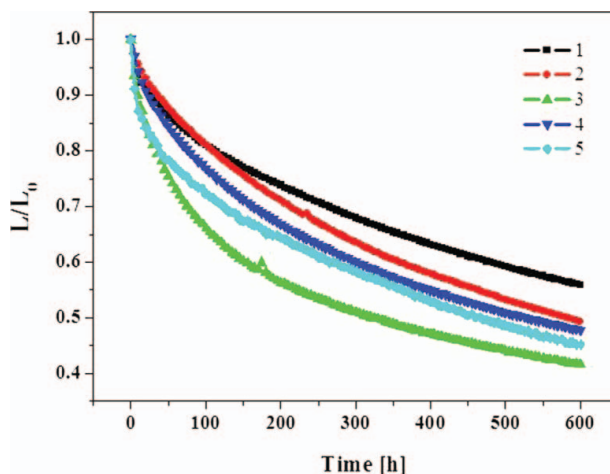


Figure 4. Operational lifetime tests for the blue devices used in this study.

luminance of devices **1–5** were 7207, 8252, 14810, 12590 and 10540 cd/m^2 , respectively. Variations in the luminous and power efficiencies of devices **1–5**, as a function of the current density, are shown in Fig. 6(a) and (b). The luminous efficiency were 6.10, 7.35, 7.23, 9.10, and 7.66 cd/A at 20 mA/cm^2 , respectively. And the power efficiencies of devices **1–5** were 2.39, 2.89, 3.21, 3.74, and 3.15 lm/W at 20 mA/cm^2 , respectively. Also, the maximum luminous/ power efficiencies of compounds **1–5** are 6.65/3.38, 8.37/4.48, 7.39/3.98, 9.66/5.35, and 7.79(cd/A)/3.88(lm/W), respectively. The EL performances are sensitive to the substituents at the 4- and 4'-positions of the central stilbene core. Notably, the efficiency of the OLED device with dopant **4** were much higher than those of dopant **1**, **2**, **3**, and **5** due to the superior matched spectral overlap between the emission of the host and the absorption of the dopant, as shown in Fig. 1(a). The maximum brightness of this device was 12590 cd m^{-2} , with a luminous efficiency of 9.10 cd A^{-1} at 20 mA cm^{-1} and power efficiency of 3.74 lm W^{-1} at 20 mA cm^{-1} . The EL parameters for blue dopant

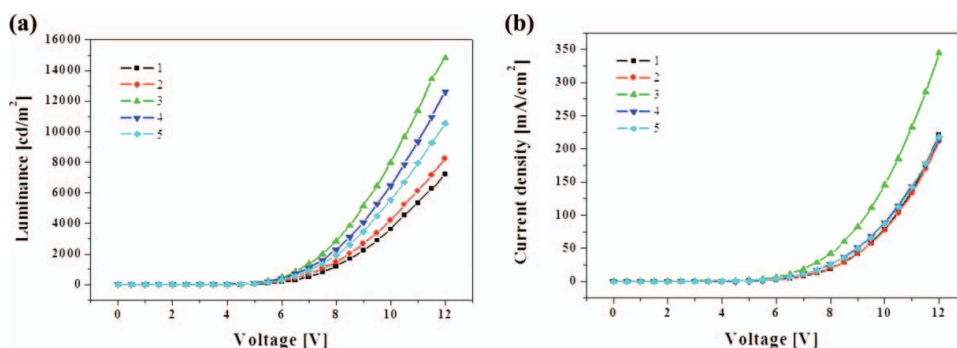


Figure 5. (a) Luminance and (b) current density versus applied electric voltage characteristics of devices **1–5**.

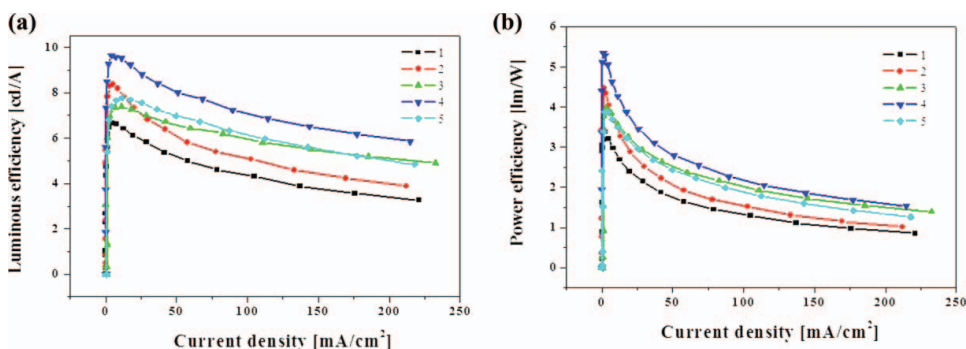


Figure 6. (a) Luminous efficiencies and (b) power efficiencies as a function of current density for the device.

4 reflect its promising application in OLED devices. This study clearly suggests that not only the high quantum yield of the dopant, but also the superior matched spectral overlap between the emission of the host and the absorption of the dopant can improve efficiencies of blue OLEDs composed of a host and dopant.

Conclusions

A series of blue-emitting materials based on a stilbene core with various arylamine groups were designed and synthesized for OLEDs. When doped in the ADN host in the OLED device, these materials showed blue electroluminescent properties. Particularly, the device **4** doped with blue dopant **4** showed the CIE coordinate of (0.155, 0.195) at 10 V, a maximum luminance of 12590 cd/m², a luminous efficiency of 9.10 cd/A at 20 mA/cm², and a power efficiency 3.74 lm/W at 20 mA/cm². These results demonstrated that these new bis(diarylamino)stilbene derivatives are promising blue dopants for OLED applications.

Acknowledgment

This research was supported by Basic Science Research Program through the NRF funded by the Ministry of Education, Science and Technology (20110004655).

References

- [1] Gymer, R. W., Holmes, A. B., Burroughes, J. H., Marks, R. N., Taliani, C., Bradley, D. D. C., Dos Santos, D. A., Bredas, J. L., Logdlund, M., & Salaneck, W. R. (1999). *Nature*, *397*, 121.
- [2] Leung, L. M., Lo, W. Y., So, S. K., Lee, K. M., & Choi, W. K. (2002). *J. Am. Chem. Soc.*, *122*, 5640.
- [3] Strukeji, M., Jordan, R. H., & Dodabalapur, A. (1996). *J. Am. Chem. Soc.*, *118*, 1213.
- [4] Kishigami, Y., Tsubaki, K., Kondo, Y., & Kido. (2005). *J. Synth. Met.*, *153*, 241.
- [5] Markham, J. P. J., Namdas, E. B., Anthopoulos, T. D., Samuel, I. D. W., Richards, G. J., & Burn, P. L. (2004). *Appl. Phys. Lett.*, *85*, 1463.
- [6] Tao, S., Peng, Z., Zhang, X., Wang, P., Lee, C.-S., & Lee, S.-T. (2005). *Adv. Funct. Mater.*, *15*, 1716.
- [7] Chen, C.-H., Wu, F.-I., Shu, C.-F., Chien, C.-H., & Tao, Y.-T. (2004). *J. Mater. Chem.*, *14*, 1585.
- [8] Fischer, A., Chenais, S., Forget, S., Castex, M.-C., Ades, D., Siove, A., Denis, C., Maise, P., & Geffroy, B. (2006). *J. Phys. D: Appl. Phys.*, *39*, 917.

- [9] Lee, K. H., You, J. N., Kwon, H. J., Kim, Y. K., & Yoon, S. S. (2010). *Mol. Cryst. Liq. Cryst.*, 530, 40.
- [10] Lee, K. H., Kang, L. K., Lee, J. Y., Kang, Y., Jeon, S. O., Yook, K. S., Lee, J. Y., & Yoon, S. S. (2010). *Adv. Funct. Mater.*, 20, 1345.
- [11] Park, J. K., Lee, K. H., Park, J. S., Seo, J. H., Kim, Y. K., & Yoon, S. S. (2010). *Mol. Cryst. Liq. Cryst.*, 531, 55.
- [12] Kim, S. O., Lee, K. H., Kang, S., Lee, J. Y., Seo, J. H., Kim, Y. K., & Yoon, S. S. (2010). *Bull. Korean Chem. Soc.*, 31, 389.
- [13] Oh, S., Lee, K. H., Seo, J. H., Kim, Y. K., & Yoon, S. S. (2011). *Bull. Korean Chem. Soc.*, 32, 1593.
- [14] Yang, J.-S., Chiuo, S.-Y., & Liau, K.-L. (2002). *J. Am. Chem. Soc.*, 124, 2518.
- [15] Li, H.-C., Lin, Y.-P., Chou, P.-T., Cheng, Y.-M., & Liu, R.-S. (2007). *Adv. Funct. Mater.*, 17, 520.
- [16] Kim, S. O., Lee, K. H., Kwon, H. J., Kim, Y. K., & Yoon, S. S. (2010). *Mol. Cryst. Liq. Cryst.*, 530, 40.
- [17] Xu, Q., Chen, H. Z., & Wang, M. (2004). *Mater. Chem. Phys.*, 87, 446.
- [18] Zhan, C., Cheng, Z., Zheng, J., Zhang, W., Xi, Y., & Qin, J. (2002). *J. Appl. Polym. Sci.*, 85, 2718.
- [19] Ho, M.-H., Wu, Y.-S., & Chen, C. H. (2005). Digest of technical papers. *SID*, 36(Bk. 1), 802.
- [20] Li, C. L., Shieh, S. J., Lin, S. C., & Liu, R. S. (2003). *Org. Lett.*, 5, 1131.
- [21] Hung, L. S., & Chen, C. H. (2002). *Mater. Sci. Eng. R*, 39, 143.